Chemical Science

Accepted Manuscript

This article can be cited before page numbers have been issued, to do this please use: Y. Wang, H. Cui, Z. Wei, H. Wang, L. Zhang and C. Su, *Chem. Sci.*, 2016, DOI: 10.1039/C6SC03288E.

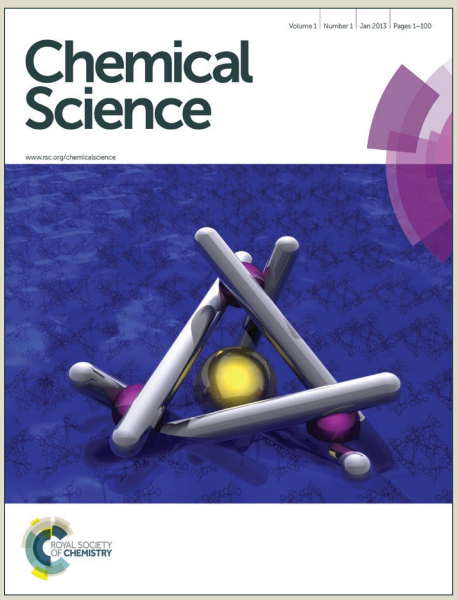

www.rsc.org/chemicalscience

View Article Online
DOI: 10.1039/C6SC03288E

Journal Name

ARTICLE

Received 00th January 20xx,
Accepted 00th January 20xx

DOI: 10.1039/x0xx00000x

www.rsc.org/

Engineering Catalytic Coordination Space in a Chemical Stable Ir-Porphyrin MOF with Confinement Effect Inverting Conventional Si-H Insertion Chemoselectivity

Yingxia Wang, Hao Cui, Zhangwen Wei, Hai-Ping Wang, Li Zhang,* and Cheng-Yong Su*

An iridium-porphyrin ligand, Ir(TCPP)Cl (TCPP = tetrakis(4-carboxyphenyl)porphyrin), has been utilized to react with $HfCl_4$ to generate a stable Ir(III)-porphyrin metal-organic framework of the formula $[(Hf_6(\mu_3\text{-}O)_8(OH)_2(H_2O)_{10})_2(Ir(TCPP)Cl)_3]\cdot$solvents (Ir-PMOF-**1**(Hf)), which possesses two types of open cavities (1.9 × 1.9 × 1.9 and 3.0 × 3.0 × 3.0 nm^3) crosslinked through orthogonal channels (1.9 × 1.9 nm^2) in three directions. The smaller cavity is surrounded by four catalytic Ir(TCPP)Cl walls to form a confined coordination space as molecular nanoreactor, while the larger one facilitates reactant/product feeding and release. Therefore, the porous Ir-PMOF-**1**(Hf) can act as multi-channel crystalline molecular flasks to promote carbenoid insertion reaction into Si-H bond, featuring high chemoselectivity towards primary silanes among primary, secondary and tertiary silanes in heterogeneous condition that is inaccessible by conventional homogeneous catalysts.

Introduction

Crystal engineering of metal-organic frameworks (MOFs) provides a powerful platform to explore their versatile potentials correlating to designable porosity and complexity.[1] In this regard, functionalization of an MOF may be realized from coordination space engineering (CSE) in MOF pores via one-pot synthesis or postmodification.[2] Thank to plentiful reticular chemistry of MOFs, engineering of coordination spaces (CSs) as the basic functional units for a specific application becomes feasible by virtue of deliberate selection of metal ion, organic linker and framework topology.[3] For example, engineering catalytic CSs in an MOF can start from design of active sites with the selectivity controllable by confinement effect from framework cavities and pore windows.

The transition-metal-catalyzed carbenoid insertion into the Si-H bond is an attractive method to prepare α-silyl carbonyl compounds. Besides dirhodium(II)[4] and copper[5] complexes which are generally superior catalysts for the carbene transfer reactions, only a few examples involving Zn,[6] Ag,[7] Au[8] and Ir[9] have been reported to catalyze Si-H insertion reactions. The majority of these catalytic reactions prefer tertiary silanes. Pérez has ever studied the relative reactivity of substituted silanes in the presence of a Cu or Ag-based catalyst, and found that these catalysts display activity order of tertiary > secondary > primary for ethyl substituted silanes, whereas an inverted order of secondary > tertiary ≈ primary for phenyl substituted silanes.[7] Nevertheless, none of the reported catalysts display the prior chemoselectivity for the primary silanes. The bond dissociation energy (BDE) of the Si-H bond is increasing along tertiary, secondary and primary silanes, and thus the primary Si-H bonds are the most inert towards the insertion reaction with carbenoids.[10] However, it was noted that a considerable steric effect could be aroused by multiply substituents in secondary and tertiary silanes. Therefore, a potential selectivity for primary silanes may be achieved if the reaction takes place in a confined space, where the active sites become more inaccessible to bulky substrates. In this context, CSE of confined and catalytic nanoreactors in MOF pores may offer an ideal whereas easy approach to such purpose owing to additional selectivity endowed by the channel size, making it possible to obtain less active primary silanes for further conversion into diverse secondary silanes with plenty of practical uses.[11]

Herein, we testify this speculation by designing a robust and self-supported iridium-porphyrinic MOF catalyst, $[(Hf_6(\mu_3\text{-}O)_8(OH)_2(H_2O)_{10})_2(Ir(TCPP)Cl)_3]\cdot$solvents (Ir-PMOF-**1**(Hf), TCPP = tetrakis(4-carboxyphenyl)porphyrin), through incorporating Ir(III)-porphyrin active sites on the pore surface to generate catalytic CSs. Owing to its continuous and permeable channels crosslinking the catalytic CSs, Ir-PMOF-**1**(Hf) behaves as multi-channel crystalline molecular flasks[12] featuring effective

MOE Laboratory of Bioinorganic and Synthetic Chemistry, Lehn Institute of Functional Materials, School of Chemistry and Chemical Engineering, Sun Yat-sen University, Guangzhou 510275, China. E-mail: zhli99@mail.sysu.edu.cn; cesscy@mail.sysu.edu.cn

† Electronic supplementary information (ESI) available: Physical characterizations of metalloporphyrin ligands, crystal structure data, physical characterizations, chemical/thermal stability study, and gas adsorption of porphyrinic MOFs, recycling experiments, and NMR data of Si-H insertion products. CIF files giving crystallographic data. CCDC 1491233. For ESI and crystallographic data in CIF or other electronic format see DOI: 10.1039/x0xx00000x.

View Article Online
DOI: 10.1039/C6SC03288E

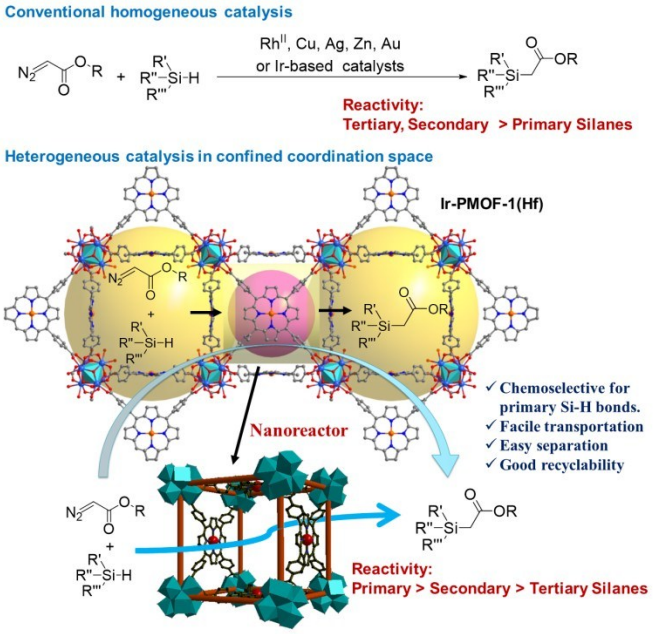

Scheme 1. Heterogeneous chemoselectivity of primary Si-H insertion induced by confined coordination space in Ir-PMOF-**1**(Hf) showing opposite reactivity order to conventional homogeneous catalysis.

confinement effect and easy transportation of reactant/product into/from inner reactive vessels.[13-24] The prior selectivity and reactivity for primary Si-H insertion reaction (Scheme 1) has been successfully established, supplementing alternative chemoselective choice in contrast to conventional homogeneous catalysts. To the best of our knowledge, this is the first report about the inverted selectivity order, i.e., primary > secondary > tertiary, for Si-H insertion induced by a metal catalyst.

EXPERIMENTAL

General Information. All the reagents in the present work were obtained from the commercial source and used directly without further purification. The metalloporphyrin ligands Ir(TCPPCO$_2$Me)(CO)Cl and Ir(TCPP)Cl were synthesized according to our recent work.[14] The elemental analyses were performed with Perkin-Elmer 240 elemental analyzer. HRESI-MS was performed by using a Bruker Daltonics ESI-Q-TOF maXis4G. Infrared spectra on KBr pellets were collected with a Nicolet/Nexus-670 FT-IR spectrometer in the region of 4000-400 cm^{-1}. UV-vis spectra were tested on a Shimadzu/UV-3600 spectrophotometer. ^{1}H and ^{13}C NMR were recorded on Bruker AVANCE III 400MHz. PXRD patterns were recorded on SmartLab X-ray powder diffractometer (Rigaku Co.) at 40 kV and 30 mA with a Cu target tube. Thermogravimetric (TG) analyses were performed under an air atmosphere at a heating rate of 2 °C min^{-1} by using a NETZSCH TG 209 system. X-ray photoelectron spectroscopy (XPS) was performed on a ULVAC PHI Quantera microprobe. Binding energies (BE) were calibrated by setting the measured BE of C 1s to 284.65 eV. The sorption isotherms for N$_2$ (77 K) gas were measured with an Autosorb-iQ2-MP gas sorption analyzer (Quantachrome, USA).

Cautions! Although we have not experienced any problem in the handling of the diazo compounds, extreme care should be taken when manipulating them due to their explosive nature.

Synthesis of ($Hf_6(\mu_3\text{-}O)_8(OH)_2(H_2O)_{10})_2(Ir(TCPP)Cl)_3$·solvents (Ir-PMOF-1(Hf)). Ir(TCPP)Cl (5 mg, 4.9×10^{-3} mmol), HfCl$_4$ (15 mg, 4.7×10^{-2} mmol), benzoic acid (400 mg, 3.27 mmol) and dimethylformamide (DMF, 1 mL) were placed in a glass vial, which was then sealed and heated to 120 °C in an oven. After 48 h, red block crystals were obtained (7 mg, 77% yield based on Ir(TCPP)Cl) and air-dried. Anal. Calcd. For ($Hf_6(\mu_3\text{-}O)_8(OH)_2(H_2O)_{10})_2(Ir(TCPP)Cl)_3\cdot 9(C_6H_5COOH)\cdot 2H_2O$ ($C_{207}H_{176}Cl_3Ir_3N_{12}O_{85}Hf_{12}$): C, 35.43; H, 2.53; N, 2.40. Found: C, 35.01; H, 3.01; N, 2.28%. FT-IR (KBr) ν 3402 (br), 1658 (s), 1601 (s), 1552 (s), 1418 (s), 1075 (m), 1015 (m), 718 (m), 664 (m) cm^{-1}.

Single X-ray Crystallography. The X-ray diffraction data was collected with an Agilent Technologies SuperNova X-RAY diffractometer system equipped with Cu-kα radiation (λ = 1.54178 Å). The crystal was kept at 150(10) K during data collection. The structure was solved with the ShelXS structure solution program integrated in Olex232 using Direct Methods, and refined with the ShelXL refinement package using CGLS minimisation.[25a] The refinement was restricted to one set of molecules by using DIFX and FLAT to constrain porphyrin ligand. ISOR/SIMU was applied to all non-hydrogen atoms to simulate isotropic behaviors. All solvent molecules have been removed by SQUEEZE program.[25b] The positions of the hydrogen atoms are generated geometrically. A summary of the crystal structure refinement data and selected bond angles and distances are listed in Table S1 and S2. CCDC 1491233.

Typical Procedure for Si-H Insertion. A solution of ethyl 2-diazoacetate (EDA, 45.6 mg, 0.4 mmol, 1.0 eq) in DCM (1.0 mL) was added slowly to the mixture of phenylsilane (PhSiH$_3$, 216.4 mg, 2.0 mmol, 5.0 eq) and activated Ir-PMOF-**1**(Hf) (6.4 mg, 0.0032 mmol, 0.8 mol [Ir]%) in dicholoromethane (DCM, 1 mL). The resulting suspension was stirred at room temperature for 3 min until EDA was completely consumed. The undissolved catalyst was removed through centrifugation, and washed with DCM (3 × 8 mL). The combined supernatant was evaporated to dryness, and the residue was dissolved in CDCl$_3$ and analyzed by ^{1}H NMR to determine the conversion of EDA to ethyl 2-(phenylsilyl)acetate (**2a**, 93%).

RESULTS AND DISCUSSION

Solvothermal reaction of Ir(TCPP)Cl and HfCl$_4$ in the presence of benzoic acid in DMF at 120°C for 48 h yielded red block crystals of Ir-PMOF-**1**(Hf). Single-crystal X-ray diffraction studies reveal that Ir-PMOF-**1**(Hf) crystallizes in cubic space group *Im*-3m as an isostructure of Ir-PMOF-**1**(Zr)[14] and PCN-224,[24] whereas based on Hf$_6$-clusters (Figure 1). The basic Hf-oxide node may consist of a core Hf$_6$(μ_3-O)$_8$ octahedron and 12 terminal H$_2$O/OH$^-$ groups, in which each vertex of Hf$_6$-octahedron is occupied by a Hf(IV) atom and each face is

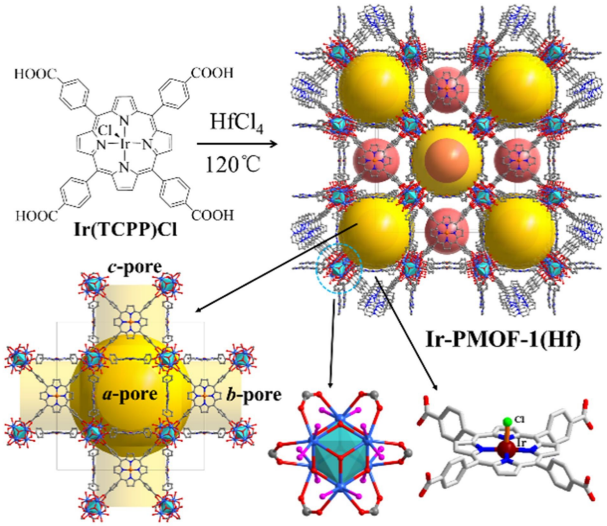

Figure 1. Assembly of 3D Ir-PMOF-**1**(Hf) based on 6-connected $Hf_6(\mu_3\text{-}O)_8(OH)_2(H_2O)_{10}$ cluster and 4-connected Ir(TCPP)Cl ligand, showing two types of cavities interconnected to generate open channels in three directions.

capped by one μ_3-oxygen atom. Six edges of the Hf_6-octahedron are bridged by carboxylates from six different 4-connecting Ir(TCPP)Cl ligands, thus leading to the formation of three-dimensional (3D) framework of (4,6)-connected **she** net. There are two types of cavities having open windows in such topological framework. One is bigger surrounded by 8 $Hf_6(\mu_3\text{-}O)_8$ clusters (3.0 × 3.0 × 3.0 nm^3) while the other is smaller enclosed by 4 Ir(TCPP)Cl (1.9 × 1.9 × 1.9 nm^3) units, which interconnect with each other to form square-like pores (1.9 × 1.9 nm^2) intercrossing in three orthogonal directions. Therefore, Ir-PMOF-**1**(Hf) can be regarded as a multi-channel platform for heterogeneous catalysis with self-supporting parallel nanoreactors and transportation channels, where catalytic Ir-porphyrin sites are confined in CSs with open windows for convenient reactant/product feeding and release.

The powder X-ray diffraction (PXRD) patterns of bulk samples closely match with the simulated one from single-crystal data, indicative of satisfactory phase purity (Figure S1). As the crystal structure of Ir-PMOF-**1**(Hf) shows, the atomic ratio of Hf : Ir : Cl is 4 : 1 : 1, which is further confirmed by energy-dispersive X-ray spectroscopy (EDS) and X-ray photoelectron spectroscopy (XPS) analyses (Figures S2-3; Tables S3-4). Two intense peaks around 65.1 and 62.2 eV appear in the XPS spectrum, which are assignable to Ir $4f_{5/2}$ and Ir $4f_{7/2}$, respectively.[26]

The thermal gravimetric (TG) curve of the desolvated Ir-PMOF-**1**(Hf) crystallites displays no obvious weight loss up to 340°C, where the framework starts to decompose (Figure S4). The variable temperature PXRD experiments disclose that the framework porosity can sustain heating up to 220°C (Figure S5). Ir-PMOF-**1**(Hf) exhibits excellent chemical stability. After immersing the fresh crystals in a wide range of solvents, such as dicholoromethane (DCM), ethyl acetate (EA), diethyl ether (Et_2O), acetonitrile (MeCN), tetrahydrofuran (THF), methanol (MeOH) and water for 3-5 days, the PXRD patterns of the

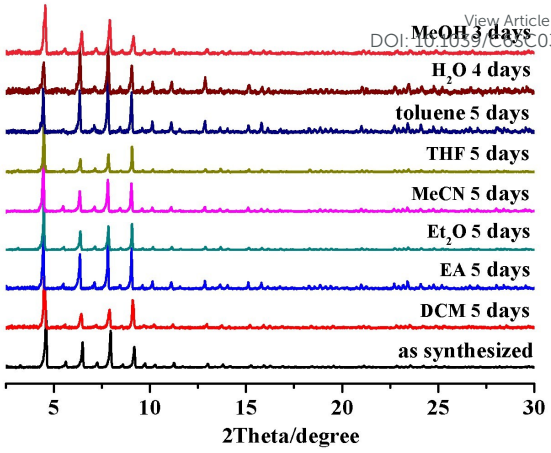

Figure 2. Stability test of Ir-PMOF-**1**(Hf) in different solvents.

recycled samples still retain the prominent peak profile and crystallinity (Figure 2), verifying that the porous Ir-PMOF-**1**(Hf) crystals are competent for heterogeneous catalysis in these solvent. After soaking the samples of Ir-PMOF-**1**(Hf) in pH = 0-11 and inorganic salts aqueous solution for 24 h, the PXRD patterns show comparable diffraction profiles with the as-synthesized sample (Figure S6).

The porosity of Ir-PMOF-**1**(Hf) has been evaluated by N_2 adsorption isotherms at 77 K (Figure S7). Prior to sorption measurement, the samples were subjected to solvent exchange with acetone for 10 h and then activated by heating at 120 °C under vacuum for 12 h. The N_2 adsorption of Ir-PMOF-**1**(Hf) shows typical type-I isotherm, indicative of micro-porosity. A N_2 uptake of 535 cm^3 g^{-1} is obtained, and the Brunauer-Emmet-Teller (BET) surface area is calculated as 1758 m^2 g^{-1}. According to Density Functional Theory (DFT) pore distribution plot of Ir-PMOF-**1**(Hf), the pore diameter of the sample is approximately 1.6 nm (Figure S8), which approximates to the single-crystal analysis (1.9 nm). As calculated by PLATON analysis, the effective solvent accessible void in the crystal lattice is 78.4% of the cell volume.

The superiority of Ir-PMOF-**1**(Hf) in Si-H insertion reaction has been examined by the model reaction of ethyl 2-diazoacetate (EDA) and phenylsilane ($PhSiH_3$). In the presence of 0.8 mol [M]% of the metal catalysts, including Ir-PMOF-**1**(Hf), Ir(TPP)(CO)Cl (TPP = 5,10,15,20-tetraphenylporphyrin) and $Rh_2(OAc)_4$, the reactions of a 1:5 molar ratio mixture of EDA and $PhSiH_3$ in DCM after 3 min produce the Si-H insertion product of ethyl 2-(phenylsilyl)acetate (**2a**) in 93, 86 and 83% yields, respectively (Table 1, entries 1-3). In each reaction, EDA was completely consumed. In addition to the Si-H insertion products, the self-coupling reaction products of EDA, i.e. diethyl fumarate and maleate account for all initial EDA. The similar reaction catalyzed by $Cu(OTf)_2$ is found ineffective, and **2a** is formed in only 41% yield after 48 h (entry 4). When decreasing the molar percent of [Ir] to 0.04%, the reaction in the presence of Ir-PMOF-**1**(Hf) still achieves 76% yield, although a much longer reaction time of 12 h is required (entry 5). Based on these catalytic results, the turnover frequency (TOF) and the turnover number (TON) of Ir-PMOF-**1**(Hf) can be

Table 1. Catalytic Si-H Insertion.[a]

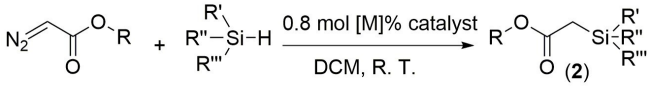

Entry	Catalyst	Time	Product	Yield(%)
1	Ir-PMOF-**1**(Hf)	3 min	**2a** 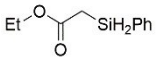	93
2	Ir(TPP)(CO)Cl	3 min	**2a**	86
3	$Rh_2(OAc)_4$	3 min	**2a**	83
4	$Cu(OTf)_2$	48 h	**2a**	41
5[b]	Ir-PMOF-**1**(Hf)	12 h	**2a**	76
6	Ir-PMOF-**1**(Hf)	6 min	**2b** 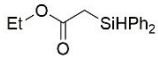	82
7	Ir-PMOF-**1**(Hf)	7 min	**2c** 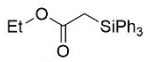	33
8	Ir-PMOF-**1**(Hf)	5 min	**2d** 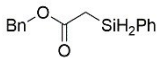	73
9	Ir-PMOF-**1**(Hf)	20 min	**2e** 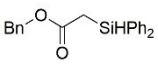	51
10	Ir-PMOF-**1**(Hf)	1 h	**2f** 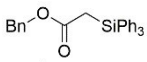	28
11	Ir-PMOF-**1**(Hf)	3 min	**2g** 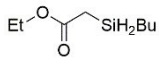	91
12	Ir-PMOF-**1**(Hf)	3 min	**2h** 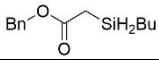	84

[a]Reaction conditions: 0.8 mol [M]% of the catalyst. The yields are based on the conversions of diazoacetates to the Si-H insertion products. In each reaction, EDA has been completely consumed. [b]Catalyst amount: 0.04 mol [Ir]%.

estimated up to 2325 h^{-1} and 1900, respectively.

Ir-PMOF-**1**(Hf) is also efficient in inducing the reaction of secondary silane. The reaction of EDA and diphenylsilane (Ph_2SiH_2) in the presence of 0.8 mol [Ir]% of Ir-PMOF-**1**(Hf) leads to the formation of ethyl 2-(diphenylsilyl)acetate (**2b**) in 82% yield (entry 6). For comparison, the Si-H insertion reaction of the tertiary silane such as triphenylsilane (Ph_3SiH) is sluggish, and the product, ethyl 2-(triphenylsilyl)acetate (**2c**), is generated in only 33% yield (entry 7). Changing the diazo compound to benzyl 2-diazoacetate (BDA), the reactions with $PhSiH_3$, Ph_2SiH_2 and Ph_3SiH give the Si-H insertion products **2d-f** in the yields of 73, 51 and 28%, respectively, and the reaction time has been lengthened from 5 min to 1 h (entries 8-10). Besides phenylsilane, other primary silanes like *n*-butylsilane ($BuSiH_3$) can also react with both of EDA and BDA in the presence of Ir-PMOF-**1**(Hf) to generate Si-H insertion products **2g** and **2h** in high yields (entries 11 and 12). After the above catalytic reactions, the PXRD patterns of the recycled catalyst samples remain almost intact, confirming that the porous framework of Ir-PMOF-**1**(Hf) can well tolerate the catalytic process (Figure S9).

Comparison among the above catalytic activities of differently substituted silanes obviously discloses a reactivity order of primary > secondary > tertiary silanes (entries 1, 6-10). This reactivity order induced by Ir-PMOF-**1**(Hf) is strikingly different from the known order of Si-H insertion homogeneously catalyzed by dirhodium(II) tetracarboxylates,[4]

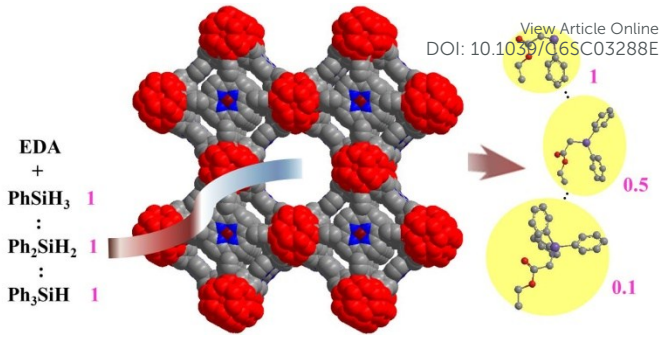

Figure 3. Chemoselective Si-H insertion heterogeneously catalysed by Ir-PMOF-**1**(Hf) framework. Numbers show molar ratio.

metalloporphyrin complexes,[9] Cu(I/II)[5] and Ag(I)[7] salts, under whose catalysis the secondary and tertiary silanes display prior activity to primary silanes.

To further evaluate the chemoselectivity of Ir-PMOF-**1**(Hf) towards primary silanes, a competition experiment has been carried out, employing a 0.9 : 1.35 : 2.7 molar ratio mixture of $PhSiH_3$, Ph_2SiH_2 and Ph_3SiH as the Si-H sources, and thus the amounts of the primary, secondary and tertiary Si-H bonds are equal (Figure S10).[7] One equivalent of EDA reacts with this mixture to give rise to Si-H products **2a-c** in the molar ratio of 1 : 0.7 : 0.3 in the presence of Ir-PMOF-**1**(Hf). In a similar way, BDA reacts with this mixture to produce **2d-f** in the molar ratio of 1 : 0.7 : 0.3. For comparison, the similar reactions induced by Ir(TPP)(CO)Cl and $Rh_2(OAc)_4$ generates **2a-c** in the ratios of 1 : 1 : 0.4 and 1 : 1.5 : 1.2, respectively. Competition experiments between two of the three silanes under the catalysis of Ir-PMOF-**1**(Hf) have also been carried out, the molar ratios of **2a** : **2b** and **2a** : **2c** are 1 : 0.7 and 1 : 0.2, respectively. Considering that the Si-H insertion products **2a-c** do not undergo further Si-H insertion in the presence of Ir-PMOF-**1**(Hf), we have also carried out a similar competition experiment but employed a 1 : 1 : 1 molar ratio mixture of $PhSiH_3$, Ph_2SiH_2 and Ph_3SiH instead. The catalytic result discovered that **2a**, **2b** and **2c** were formed in the molar ratio of 1 : 0.5 : 0.1 (Figure 3).

The inverted chemoselectivity for the carbenoid insertion into primary Si-H bonds induced by Ir-PMOF-**1**(Hf) may be ascribed to the following two reasons. On one hand, the active sites are located on the axial positions of the metalloporphyrin motifs which enclose a confined nanospace, imposing more steric effect toward bulky reactants than free metal catalysts such as dirhodium(II) tetracarboxylates. As a result, the sterically unfavored tertiary silanes display poor chemoselectivity in case of the heterogeneous catalyst Ir-PMOF-**1**(Hf) compared to the similar metalloporphyrin-based homogeneous catalyst Ir(TPP)(CO)Cl. On the other hand, the porosity of Ir-PMOF-**1**(Hf) brings additional size selectivity and channel diffusion difference to enforce the confinement effect; therefore, the least bulky primary silane and its corresponding Si-H insertion product can be transported through the multi-channels of the self-supported catalytic Ir-PMOF-**1**(Hf) easily than those of secondary and tertiary analogues. The overall result might explain the high chemoselectivity and reactivity

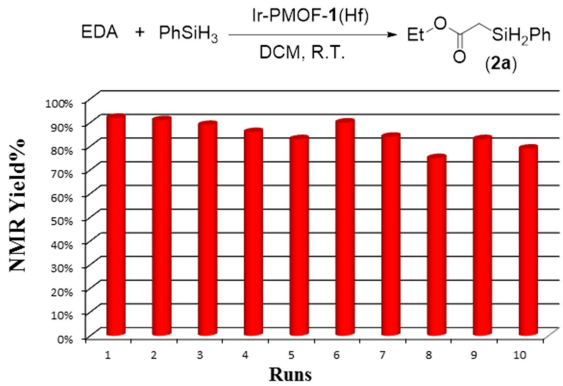

Figure 4. Recycling experiments

towards primary silanes in the Ir-PMOF-**1**(Hf)-catalyzed heterogeneous Si-H insertion reactions.

Moreover, the crystalline catalysts can be easily isolated by centrifugation, and reused at least ten times for Si-H insertion of $PhSiH_3$ with EDA (Figure 4; Table S5). During the ten reaction runs, the yields of **2a** were in the range of 74-92%. From the 1st to 6th run, it took less than 15 min to finish the reaction, whereas the 7th, 8th and 9th run needed 26, 55 and 90 min, respectively, to complete. The reduced activity from 7th run might be due to the reactants and products stucked in the pores of the Ir-PMOF-**1**(Hf) framework. In order to remove the adsorbed organic compounds in the interior and exterior surfaces during the catalytic reactions, the recycled Ir-PMOF-**1**(Hf) catalyst should be washed with DCM (3 × 8 mL) before the successive runs. The PXRD patterns of the recycled catalyst after the 1st, 3rd, 5th and 10th runs show comparable diffraction profile with the as-synthesized sample (Figure S11).

Conclusions

In summary, we have successfully imparted outstanding carbenoid transfer catalysis of homogeneous Ir-porphyrin to a porous, robust and stable Ir-PMOF-**1**(Hf), underlying a new field of heterogeneous MOF catalysis via introducing rarely explored noble metal-porphyrins (e.g. Ir, Ru and Rh). Engineering of confined and catalytic CSs in an MOF, in collaboration with its open porosity, presents multi-channel crystalline nanoreactors for selective Si-H insertion, offering higher efficiency than the corresponding homogeneous catalysts with excellent TOF and TON. An inverted reactivity and selectivity order of Si-H insertion reaction, i.e. primary > secondary > tertiary, which is unattainable by conventional metal catalysts, is achieved, and the self-supported catalyst is easy to recycle and separate. These results demonstrate the versatility of MOF catalysis that can not only incorporate excellent features of homogeneous catalysts, but also endow metal catalysis with uniqueness in heterogeneous conditions to accomplish catalytic process unachievable by homogeneous catalysts.

Acknowledgements

This work was supported by the 973 Program (2012CB821701), the NSFC Projects (21373278, 91222201), the STP Project of Guangzhou (15020016), the NSF of Guangdong Province (S2013030013474), the RFDP of Higher Education of China (20120171130006) and the Fundamental Research Funds for the Central Universities.

Notes and references

1 (a) G. Férey, *Chem. Soc. Rev.,* 2008, **37**, 191; (b)T. Devic and C. Serre, *Chem. Soc. Rev.,* 2014, **43**, 6097; (c) Z. Fang, B. Bueken, D. E. De Vos and R. A. Fischer, *Angew. Chem. Int. Ed.,* 2015, **54**, 7234; (d) A. Schneemann, V. Bon, I. Schwedler, I. Senkovska, S. Kaskel and R. A. Fischer, *Chem. Soc. Rev.,* 2014, **43**, 6062; (e) H. Furukawa, K. E. Cordova, M. O'Keeffe and O. M. Yaghi, *Science,* 2013, **341**, 1230444; (f) S. Horike, S. Shimomura and S. Kitagawa, *Nat. Chem.,* 2009, **1**, 695; (g) J. Liu, L. Chen, H. Cui, J. Zhang, L. Zhang and C.-Y. Su, *Chem. Soc. Rev.,* 2014, **43**, 6011; (h) J. Gascon, A. Corma, F. Kapteijn, F. X. Llabrés i Xamena, *ACS Catal.,* 2014, **4**, 361.

2 (a) S. Kitagawa and R. Matsuda, *Coordin. Chem. Rev.,* 2007, **251**, 2490; (b) R. A. Fischer and C. Wöll, *Angew. Chem. Int. Ed.,* 2008, **47**, 8164. (c) S. M. Cohen, *Chem. Rev.,* 2012, **112**, 970.

3 M. O'Keeffe, M. A. Peskov, S. J. Ramsden and O. M. Yaghi, *Acc. Chem. Res.,* 2008, **41**, 1782.

4 (a) H. M. L. Davies, T. Hansen, J. Rutberg and P. R. Bruzinski, *Tetrahedron Lett.,* 1997, **38**, 1741; (b) S. Kitagaki, M. Kinoshita, M. Takeba, M. Anada and S. Hashimoto, *Tetrahedron: Asymmetry,* 2000, **11**, 3855; (c) R. T. Buck, D. M. Coe, M. J. Drysdale, L. Ferris, D. Haigh, C. J. Moody, N. D. Pearson and J. B. Sanghera, *Tetrahedron: Asymmetry,* 2003, **14**, 791.

5 (a) L. A. Dakin, S. E. Schaus, E. N. Jacobsen and J. S. Panek, *Tetrahedron Lett.,* 1998, **39**, 8947; (b) Y.-Z. Zhang, S.-F. Zhu, L.-X. Wang and Q. L. Zhou, *Angew. Chem. Int. Ed.* 2008, **47**, 8496.

6 R. Vicente, J. González, L. Riesgo, J. González and L. A. López, *Angew. Chem. Int. Ed.,* 2012, **51**, 8063.

7 M. J. Iglesias, M. C. Nicasio, A. Caballero, P. J. Pérez, *Dalton Trans.,* 2013, **42**, 1191.

8 J. Ma, H. Jiang and S. Zhu, *Org. Lett.,* 2014, **16**, 4472.

9 (a) Y. Yasutomi, H. Suematsu and T. Katsuki, *J. Am. Chem. Soc.,* 2010, **132**, 4510; (b) J.-C. Wang, Z.-J. Xu, Z. Guo, Q.-H. Deng, C.-Y. Zhou, X.-L. Wan and C.-M. Che, *Chem. Commun.,* 2012, **48**, 4299.

10 Y.-D. Wu and C.-L. Wong, *J. Org. Chem.,* 1995, **60**, 821.

11 (a) D. Mukherjee, R. R. Thompson, A. Ellern and A. D. Sadow, *ACS Catal.,* 2011, **1**, 698; (b) D. Peng, Y. Zhang, X. Du, L. Zhang, X. Leng, M. D. Walter and Z. Huang, *J. Am. Chem. Soc.,* 2013, **135**, 19154; (c) M. Zhao, W. Xie and C. Cui, *Chem. Eur. J.,* 2014, **20**, 9259.

12 Y. Inokuma, M. Kawano and M. Fujita, *Nat. Chem.,* 2011, **3**, 349.

13 (a) L. Chen, T. Yang, H. Cui, T. Cai, L. Zhang and C.-Y. Su, *J. Mater. Chem. A,* 2015, **3**, 20201; (b) T. Yang, H. Cui, C. Zhang, L. Zhang and C.-Y. Su, *Inorg. Chem.,* 2013, **52**, 9053; (c) T. Yang, H. Cui, C. Zhang, L. Zhang and C.-Y. Su, *ChemCatChem,* 2013, **5**, 3131.

14 H. Cui, Y. Wang, Y. Wang, Y.-Z. Fan, L. Zhang and C.-Y. Su, *CrystEngComm,* 2016, **18**, 2203.

15 B. J. Burnett, P. M. Barron, C. Hu and W. Choe, *J. Am. Chem. Soc.,* 2011, **133**, 9984.

16 Y. Zhao, N. Kornienko, Z. Liu, C. Zhu, S. Asahina, T.-R. Kuo, W. Bao, C. Xie, A. Hexemer, O. Terasaki, P. Yang and O. M. Yaghi, *J. Am. Chem. Soc.,* 2015, **137**, 2199.

View Article Online
DOI: 10.1039/C6SC03288E

17 S. Takaishi, E. J. DeMarco, M. J. Pellin, O. K. Farha and J. T. Hupp, *Chem. Sci.,* 2013, **4**, 1509.
18 X.-L. Yang, M.-H. Xie, C. Zou, Y. He, B. Chen, M. O'Keeffe and C.-D. Wu, *J. Am. Chem. Soc.,* 2012, **134**, 10638.
19 L. Meng, Q. Cheng, C. Kim, W.-Y. Gao, L. Wojtas, Y.-S. Chen, M. J. Zaworotko, X. P. Zhang and S. Ma, *Angew. Chem. Int. Ed.,* 2012, **51**, 10082.
20 A. Fateeva, P. A. Chater, C. P. Ireland, A. A. Tahir, Y. Z. Khimyak, P. V. Wiper, J. R. Darwent and M. J. Rosseinsky, *Angew. Chem. Int. Ed.,* 2012, **51**, 7440.
21 J. A. Johnson, J. Luo, X. Zhang, Y.-S. Chen, M. D. Morton, E. Echeverría, F. E. Torres and J. Zhang, *ACS Catal.,* 2015, **5**, 5283.
22 J. Zheng, M. Wu, F. Jiang, W. Su and M. Hong, *Chem. Sci.,* 2015, **6**, 3466.
23 Q. Lin, X. Bu, A. Kong, C. Mao, X. Zhao, F. Bu and P. Feng, *J. Am. Chem. Soc.,* 2015, **137**, 2235.
24 D. Feng, W.-C. Chung, Z. Wei, Z.-Y. Gu, H.-L. Jiang, Y.-P. Chen, D. J. Darensbourg and H.-C. Zhou, *J. Am. Chem. Soc.,* 2013, **135**, 17105.
25 (a) O. V. Dolomanov, L. J. Bourhis, R. J. Gildea, J. A. K. Howard and H. J. Puschmann, *Appl. Cryst.*, 2009, **42**, 339. (b) P. V. D. Sluis and A. L. Spek, *Acta Cryst. Sect. A: Found. Crystallogr.*, 1990, **46**, 194.
26 T. V. Voskobojnikov, E. S. Shpiro, H. Landmesser, N. I. Jaeger and G. Schulz-Ekloff, *J. Mol. Catal. A-Chem.*, 1996, **104**, 299-309.